

Data models for the Compton camera acquisition and their influence on the reconstructed images

Voichița Maxim, Xavier Lojacono, Estelle Hilaire (CREATIS)
Jean-Luc Ley, Denis Dauvergne, Etienne Testa (IPNL)

Université de Lyon, France

Geneva, February 10-14, 2014



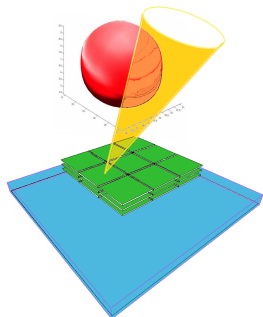
Summary

- 1 SPECT imaging with the Compton camera
- 2 From the events to the image : the system matrix
- 3 Image reconstruction : list-mode MLEM algorithm
- 4 Numerical results

Summary

- 1 SPECT imaging with the Compton camera
- 2 From the events to the image : the system matrix
- 3 Image reconstruction : list-mode MLEM algorithm
- 4 Numerical results

SPECT imaging with the Compton camera



- **Source of γ particles** : emission at some point V_0 and initial energy E
- **Scatterer** : first interaction (Compton scattering) at some V_1 and energy transmitted to an electron denoted E_1
- **Absorber** : second interaction at some V_2 (photoelectric absorption) and energy E_2
- **Projection pattern** : integral on the surface of a cone

For multiple scatterings, V_2 is the second Compton interaction and E_2 estimates $E - E_1$.

$$\cos \beta = 1 - \frac{m_e c^2 E_1}{(E - E_1)E}$$

(Compton scattering angle)

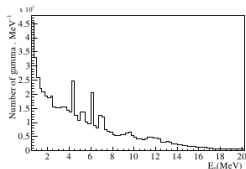
Event $\mathcal{E} = (V_1, V_2, E_1, E_2)$

associated to a Compton cone $\mathcal{C}(V_1, V_2, \beta)$

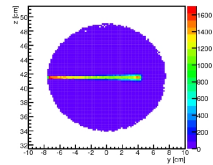
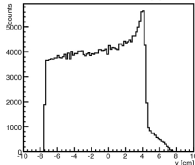
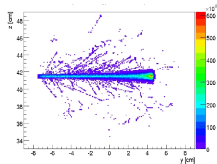
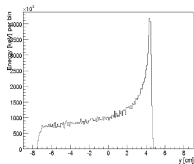
Applications

The sensitivity of the Compton camera is superior to the one of the Anger camera by 1-2 orders of magnitude.

- Imaging of poly-energetic sources
- Imaging of sources with energies ~ 1 MeV
- 3D imaging with a single camera



Emission spectrum of prompt- γ particles between 0.5 and 20 MeV obtained with a carbon ion beam at 350 MeV/u irradiating a water phantom with 10^8 ions.



PMMA-sphere irradiated by a proton beam (140 MeV), Edep.

Last interaction of γ particles that escape the phantom.

(“A tracking Compton-scattering imaging system for hadron therapy monitoring”, M. Frandes, A. Zoglauer, V. Maxim, R. Prost, IEEE TNS, 2010)

Summary

- 1 SPECT imaging with the Compton camera
- 2 From the events to the image : the system matrix
- 3 Image reconstruction : list-mode MLEM algorithm
- 4 Numerical results

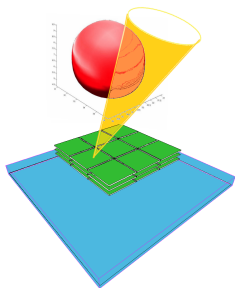
Challenge : from the events to the image

Requires a model for the conditional probability of $e = (V_1, V_2, E_1, E_2)$ given the emission point V_0 ,

$$p(\mathcal{E} = e | V_0).$$

We choose to focus on the geometrical parameters and to ignore the influence of scattering/absorption probabilities. When real positions of interaction and real energies are supposed to be measured,

$$p(\mathcal{E} = e | V_0) \propto K(\beta, E) \frac{\cos(\theta)}{V_0 V_1^2} \frac{\cos(\alpha)}{V_1 V_2^2} \delta(\beta - \beta_{V_1 V_2}),$$



$$\theta = (\overrightarrow{V_1 V_0}, \vec{n})$$

$$\alpha = (\overrightarrow{V_2 V_1}, \vec{n})$$

$$\beta_{V_1 V_2} := (\overrightarrow{V_1 V_2}, \overrightarrow{OV_1})$$

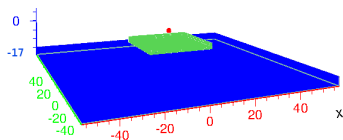
Numerical validation by simulations?

Simulation setup

Camera : three Si layers, $32 \times 32 \times 0.5 \text{ cm}^3$,
altitude $z \in \{-5, -6, -7\}$,
absorber made of $0.5 \times 0.5 \times 4 \text{ cm}^3$ crystals
at $z = -17$

Source : mono-energetic (364 keV) point
source in $O(0,0,0)$, 10^8 emitted photons.

Events : $\approx 7 \times 10^6$



Ideal detectors :

- $E_1 + E_2 = E \rightarrow e := (V_1, V_2, \beta)$
- The sequence of interactions is known
- The (x, y) positions of interaction are measured without noise; the z coordinate is taken at half-depth of the detector.

The number of events/bin ($\approx 1 \text{ mm}$, $\approx 1^\circ$) is statistically small.

Averaging

- 1 Selection of events having $z_{V_1} = -5$ cm and $z_{V_2} = -6$ cm.
- 2 For each $r_1 \in (0, 16$ cm), selection of $V_1 \in C(O_1, r_1)$ parametrized by $\varphi_1 \in [0, 2\pi)$.
- 3 For each V_1 and for each $r_2 \in (0, 8$ cm), selection of $V_2 \in C(W_2, r_2)$ parametrized by $\varphi_2 \in [0, 2\pi)$.
- 4 For each V_1, V_2 there is one single β such that $V_0 \in \mathcal{C}(V_1, V_2, \beta)$

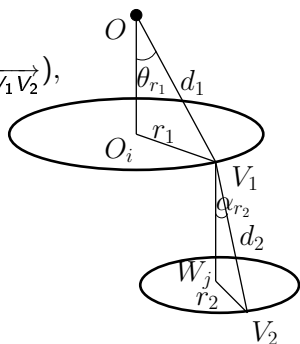
When

$$p(V_1, V_2, \beta | V_0) \propto K(\beta, E) \frac{\cos(\theta)}{V_0 V_1^2} \frac{\cos(\alpha)}{V_1 V_2^2} \delta(\beta - \beta_{V_1 V_2}),$$

$$\sum_{V_1 \in C(O_1, r_1)} \sum_{V_2 \in C(W_2, r_2)} \sum_{\beta} \frac{\hat{p}_i(V_1, V_2, \beta | V_0)}{K(\beta, E)}$$

should be proportional to

$$M(r_1, r_2) = r_1 r_2 \frac{\cos(\theta_{r_2})}{d_1^2} \frac{\cos(\alpha_{r_1})}{d_2^2}.$$



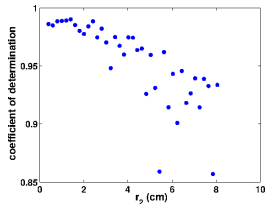
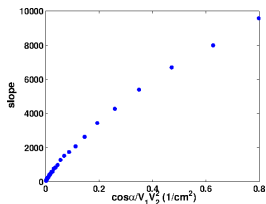
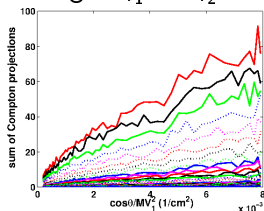
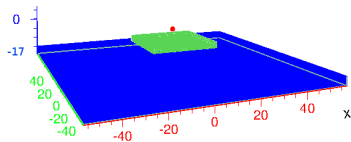
Numerical investigation

Camera : three Si layers $z \in \{-5, -6, -7\}$,
absorber at $z = -17$

Source : mono-energetic (364 keV) point
source in $O(0,0,0)$, 10^8 emitted particles

Events : $\approx 7 \times 10^6$

Binning : $d_{r_1} = d_{r_2} = 2$ mm, $d_\beta = 3^\circ$



Variation of $\frac{M(r_1, r_2)}{r_1 r_2}$
w.r. to $\frac{\cos \theta_{r_1}}{d_1^2}$;
Each r_2 : a curve

Slope from regression
as function of $\frac{\cos \alpha_{r_2}}{d_2^2}$;
Each r_2 : a point

Quality of the regression.
Degrades as V_2 moves tw.
the border.

Summary

- 1 SPECT imaging with the Compton camera
- 2 From the events to the image : the system matrix
- 3 Image reconstruction : list-mode MLEM algorithm
- 4 Numerical results

Image reconstruction : LM-MLEM algorithm

$$\widehat{\lambda}_j^{(\ell+1)} = \frac{\widehat{\lambda}_j^{(\ell)}}{s_j} \sum_i \frac{t_{ij}}{\sum_k t_{ik} \widehat{\lambda}_k^{(\ell)}}$$

where t_{ij} is the probability for a photon emitted by the voxel j to be detected as event e_i ,

$$t_{ij} = p(\mathcal{E} = e_i | v_j)$$

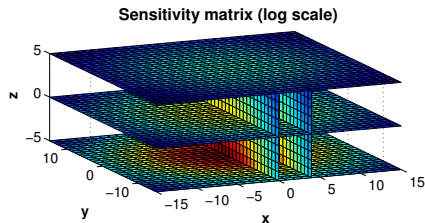
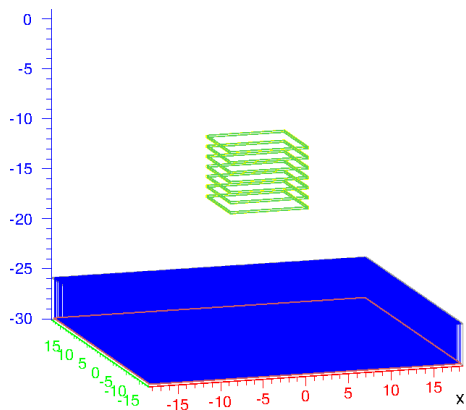
and s_j is the probability for a photon emitted by the voxel j to be detected. Thus,

$$s_j = \sum_i t_{ij}$$

where the sum is taken on all possible events, not only on the realized ones. We take

$$t_{ij} = \frac{\cos(\alpha_i)}{V_1 V_2^2} \int_{M \in v_j} K(\beta_M, E) \frac{\cos(\theta_M)}{V_1 M^2} g(\beta_M | \beta_i, \sigma_{\beta_i}) dv.$$

Sensitivity matrix



- Si scatterers, $9 \times 9 \times 0.2 \text{ cm}^3$, 128×128 strips, energy resolution 2.35 keV FWHM
- absorber in LYSO crystals, $0.5 \times 0.5 \times 4 \text{ cm}^3$, energy resolution function of the energy of the incident particle, 31 keV @ 1 MeV.

Summary

- 1 SPECT imaging with the Compton camera
- 2 From the events to the image : the system matrix
- 3 Image reconstruction : list-mode MLEM algorithm
- 4 Numerical results

Aim

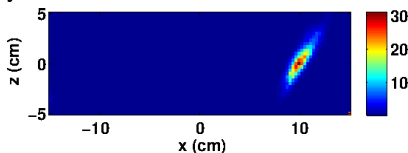
- 1 Role of the parameters of the system matrix
- 2 Role of the sensitivity matrix
- 3 Joint influence of the system matrix and of the sensitivity

Joint influence of the model and sensitivity

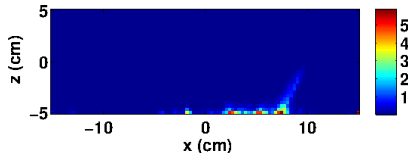
Mono-energetic (1275 keV) simulated point source in (10,0,0).

No energy selection, 3500 events, 20 iterations.

- System matrix from the model :

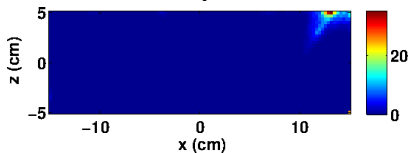


s_j from MC simulation

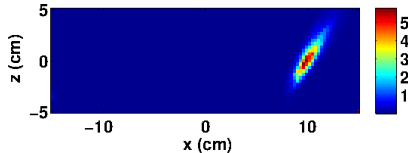


$s_j \equiv 1$

- Elements of the system matrix set to one :



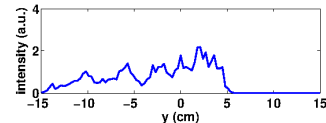
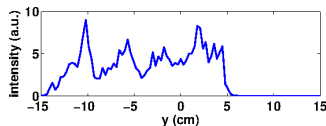
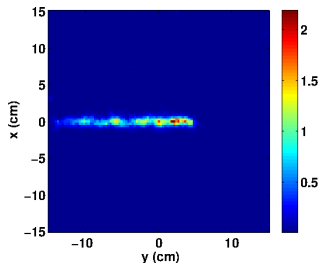
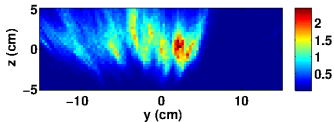
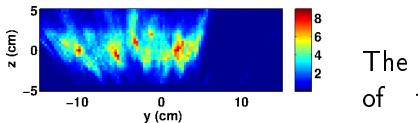
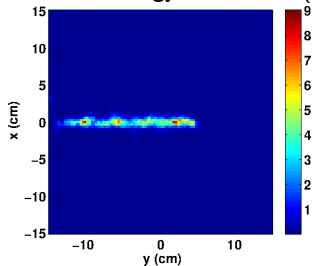
s_j from MC simulation



$s_j \equiv 1$

Is the model of the system matrix gainful?

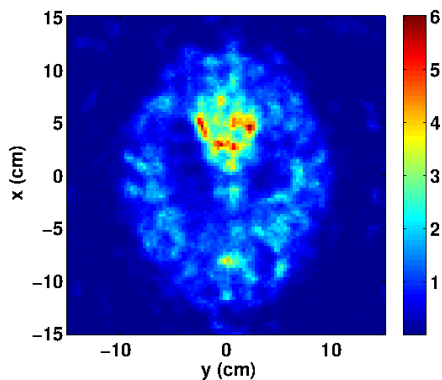
Mono-energetic (1275 keV) line source ($y \in [-14, 5]$) at 10 cm from the camera. Energy selection (20%), 6000 events, 20 iterations.



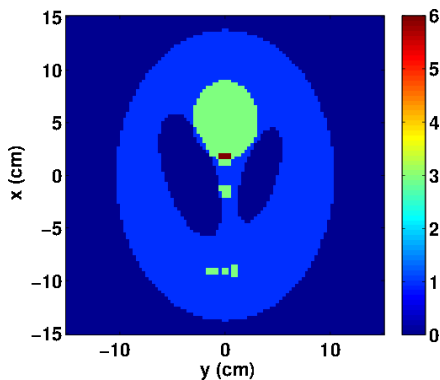
The 3D image of the source was calculated on the base of the proposed model (upper image from each pair), then with $t_{ij} \equiv 1$ and $s_j \equiv 1$ (lower image from each pair).

Examples

Mono-energetic (1275 keV) Shepp-Logan phantom at 10 cm from the camera. Energy selection (20%), 80000 events, 20 iterations.



Reconstructed image.
Horizontal slice
at 10 cm from the camera.



Original phantom (2D)

Conclusions

- The quality of the Compton images are strongly related to the models chosen for the system matrix and to the sensitivity matrix.
- The proposed theoretical model of the system matrix for ideal detectors is confirmed by simulations.
- Variants of the iterative reconstruction algorithm may improve the quality of the images.

This work was supported in part by the ENVISION Project co-funded by the European Commission under the FP7 Collaborative Projects, in part by the ETOILE Research Program PRRH/UCBL, and in part by the LABEX PRIMES of the Université de Lyon.